STATE-OF-THE-ART PAPERS

Cardiovascular Magnetic Resonance in Patients With Myocardial Infarction

Current and Emerging Applications

Han W. Kim, MD,*† Afshin Farzaneh-Far, MD, PhD,*† Raymond J. Kim, MD*†‡

Durham, North Carolina

In patients with known or suspected myocardial infarction (MI), cardiovascular magnetic resonance (CMR) provides a comprehensive, multifaceted view of the heart. The data, including that from a recent multicenter clinical trial, indicate that delayed-enhancement cardiac magnetic resonance imaging (DE-CMR) is a well-validated, robust technique that can be easily implemented on scanners that are commonly available worldwide, with an effectiveness that clearly rivals the best available imaging techniques for the detection and assessment of acute and chronic MI. When patients present outside the diagnostic window of cardiac troponins, DE-CMR may be especially useful. Moreover, because DE-CMR can uniquely differentiate between ischemic and various nonischemic forms of myocardial injury, it may be helpful in cases of diagnostic uncertainty, such as in patients with classical features of MI in whom coronary angiography does not show a culprit lesion. Even after the diagnosis of MI has been made, CMR provides clinically relevant information by identifying residual viability, microvascular damage, stunning, and right ventricular infarction. In addition, post-MI sequelae, including left ventricular thrombus and pericarditis, are easily identified. Given that quantification of infarct size by DE-CMR is highly reproducible, this technique may provide a useful surrogate end point for clinical trials with appreciable reductions in sample size compared with alternative methods.   (J Am Coll Cardiol 2010;55:1–16) © 2010 by the American College of Cardiology Foundation

Myocardial infarction (MI) is a leading cause of death worldwide (1). Accordingly, preventative and therapeutic strategies are aimed at reducing its occurrence and adverse consequences. New serological biomarkers, such as troponins, have radically improved the diagnosis of MI and have enabled the recognition of a group of patients with small infarcts, many of whom would not have been identified in earlier eras (2). Reclassifying this group as patients with MI has significant implications (2–4). From an epidemiological perspective, a substantial increase in the number of patients diagnosed with MI creates difficulties in comparing the results of new trials with those of older ones and confounds efforts to monitor the impact of public health measures and treatments. In some clinical trials, the results may be significantly altered because the diagnosis of MI can be used as an entry criterion, an end point, or both. For individual patients, the label of MI can affect a wide range of issues, including employment, disability claims, insurance, and psychological well-being. Importantly, the diagnosis of MI also impacts clinical management, and the available data indicate that even small infarcts portend worse short- and long-term prognosis (5).

Despite the use of improved biomarkers, the diagnosis of MI can still be difficult. There is marked heterogeneity in the presentation of MI and significant overlap with other disorders that result in myocardial injury, such as myocarditis and Takotsubo cardiomyopathy. In this context, it is noteworthy that the latest consensus guidelines defining MI include noninvasive imaging because it may be helpful in cases of uncertainty (6). The new criteria incorporating imaging evidence of MI involve not only established modalities such as echocardiography and radionuclide imaging, but also the newer modalities, cardiovascular magnetic resonance (CMR) and cardiac computed tomography. In particular, delayed enhancement (DE)-CMR appears to offer advantages in detecting small or subendocardial infarcts with high accuracy and is well validated (7–12). Thus, it is timely to review the role of CMR in the diagnosis and assessment of MI. In this article, we examine the utility of CMR in patients with known or suspected MI with emphasis on the additive clinical information it may provide. Additionally, there has been growing interest in using infarct size measured by CMR as an end point for clinical trials, and we discuss operational and other relevant issues for this application.

CMR

Multitechnique imaging. At the outset, it is important to recognize that CMR is not a single entity, but consists of multiple distinct techniques, each providing separate pieces of information. These different techniques arise from special software programs, called pulse sequences, and many innovations in CMR arise as much from novel pulse sequences as from advances in hardware. Thus, with different pulse sequences, each tuned to highlight specific biological tissues or properties (e.g., fat, thrombus, infarction, chamber blood flow, tissue perfusion, and so on), one can get multiple data acquisitions of the same location and obtain a comprehensive, multifaceted view of the heart (13). Additionally, because many image artifacts are pulse-sequence specific, these are not propagated throughout the examination and generally do not reduce overall scan quality (14).

The versatility of CMR, however, results in increased complexity. For each pulse sequence there are many parameters that need to be set correctly to achieve optimal image quality. Additionally, it may be unclear which pulse sequence or (more commonly) group of sequences should be used for a given clinical indication. If a pulse sequence is not performed during the scan, the image data cannot be obtained later via post-processing. As a result, standardized protocols are useful for ensuring comprehensive examinations (15). Unfortunately, at present, CMR examinations often vary among sites, even for specific indications such as MI. The rapid pace of development in pulse sequences exacerbates this problem.

Figure 1 illustrates many of the components, along with a timeline, of a typical multitechnique CMR protocol for cardiac imaging. Sequences are added or excluded depending on the indication, patient considerations (such as the ability to breath-hold), and even findings during the examination itself. Generally, all patients undergo cine imaging for the assessment of morphology, ventricular volumes, and contractile function. Delayed-enhancement imaging after gadolinium administration is routinely performed and allows the diagnosis and sizing of MI, assessment of viability, and other tissue characterization such as identification of thrombus and nonischemic scarring. Irregular heart rhythm may necessitate the use of single-shot (real-time) sequence variants to obtain diagnostic-quality images (16,17). Optional elements include stress perfusion imaging to evaluate ischemia and velocity-encoded imaging for the assessment of hemodynamics and valvular function. Additionally, T2-weighted imaging has shown promise in assessing acute, inflammatory processes such as acute MI or myocarditis, and
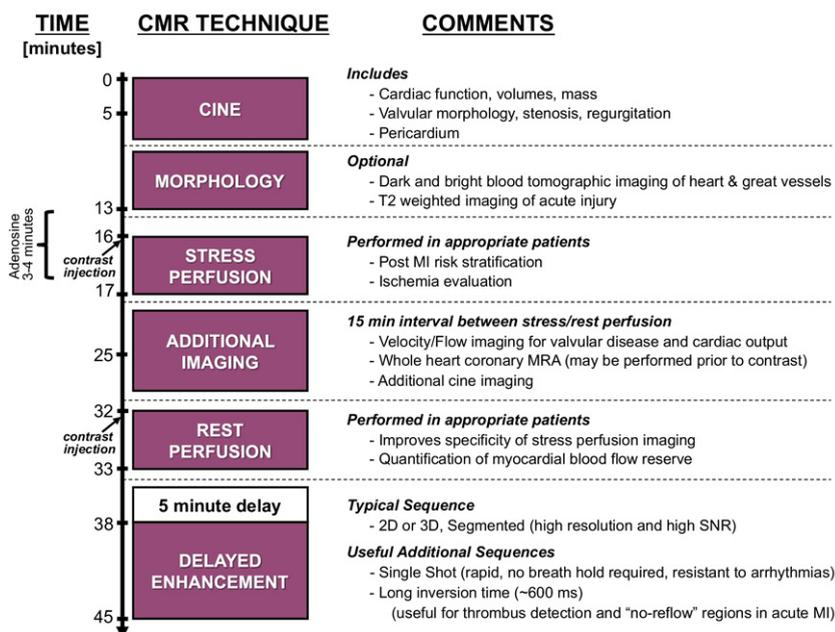

Figure 1   Timeline and Potential Components of a Multitechnique CMR Examination for Cardiac Imaging

2D = 2-dimensional; 3D = 3-dimensional; CMR = cardiovascular magnetic resonance;
MI = myocardial infarction; MRA = magnetic resonance angiography; SNR = signal-to-noise ratio.

may prove useful in distinguishing chronic lesions from those of recent onset (18). At experienced centers, coronary magnetic resonance angiography may be performed to exclude left main or 3-vessel coronary artery disease (CAD) in selected patients or to evaluate coronary anomalies (19,20).

Even in a 30- to 45-min examination, there are often a large number of data acquisitions (~50) using different techniques across multiple spatial locations. The following URL (http://dcmrc.duhs.duke.edu/figure/, Online Fig. 1) shows images from a comprehensive study and highlights the importance of side-by-side viewing of different techniques to allow efficient and accurate interpretation. The strengths and limitations of each of the different CMR techniques should be recognized when considering which to use during the examination as well as during the interpretation. The levels of experimental and clinical validation vary among techniques, and some are still undergoing development or lack the robustness necessary for general clinical use. Finally, as with any procedure, the risks of CMR must be weighed against the benefits, and patients with contraindications to magnetic resonance imaging or gadolinium contrast, such as those with pacemakers/defibrillators (21) or advanced kidney disease (owing to the risk of developing nephrogenic systemic fibrosis [22]) are not infrequently encountered.

DE. Although several CMR techniques could be used for the diagnosis of MI, the most accurate and best validated is DE-CMR. The technique is straightforward. It involves inversion-recovery imaging after intravenous administration of gadolinium contrast and a 5- to 10-min delay (23,24). With appropriate settings, normal myocardium appears black or nulled, whereas nonviable regions appear bright or hyperenhanced. The mechanism of hyperenhancement has not been fully elucidated, but one has been proposed (25) that is based on 2 simple facts. First, in normal myocardium, because myocytes are densely packed, tissue volume is predominately intracellular (~75% to 80%) (26). Second, gadolinium chelates are extracellular agents that cannot cross intact sarcolemmal membranes (27). It then follows that gadolinium distribution volume is small and tissue concentration is low in a voxel of normal myocardium. With acute necrosis (acute MI, myocarditis, and so on), there is membrane rupture, which allows gadolinium to diffuse into myocytes. This results in increased gadolinium concentration (28), shortened T1 relaxation, and thus hyperenhancement. In the chronic setting, scar has replaced necrotic tissue and the interstitial space is expanded. This again leads to increased gadolinium concentration (28) and hyperenhancement. In both acute and chronic settings (and all stages in between), one can consider viable myocytes as actively excluding gadolinium. Thus, the unifying mechanism of hyperenhancement appears to be the absence of viable myocytes rather than any inherent properties that are specific for acute necrosis, collagenous scar, or other forms of nonviable myocardium (25). In the literature, the technique of DE imaging is also known as delayed hyperenhancement, myocardial delayed enhancement, late gadolin-

ium enhancement, and simply contrast-enhanced CMR. Concerning late gadolinium enhancement, we note that other T1-shortening contrast media aside from gadolinium could show late enhancement.

In animal models, extensive comparisons have shown a nearly exact relationship between the size and shape of infarcted myocardium by DE-CMR to that of histopathology (Fig. 2A) (7,8,28–33). Additionally, these studies show that DE-CMR can distinguish between reversible and irreversible injury independent of wall motion, infarct age, and reperfusion status. Studies in humans have shown that infarct size measured by DE-CMR is closely associated with peak cardiac enzyme release (10,34–38) and measurements by positron emission tomography (39,40). DE-CMR also appears to be superior to single-photon emission computed tomography (SPECT) in detecting subendocardial infarcts and infarcts in nonanterior locations (8,11). Furthermore, the high spatial resolution of DE-CMR enables visualization of even microinfarctions, involving as little as 1 g of tissue, which may occur during otherwise successful percutaneous coronary intervention (Fig. 2B) (9,10).
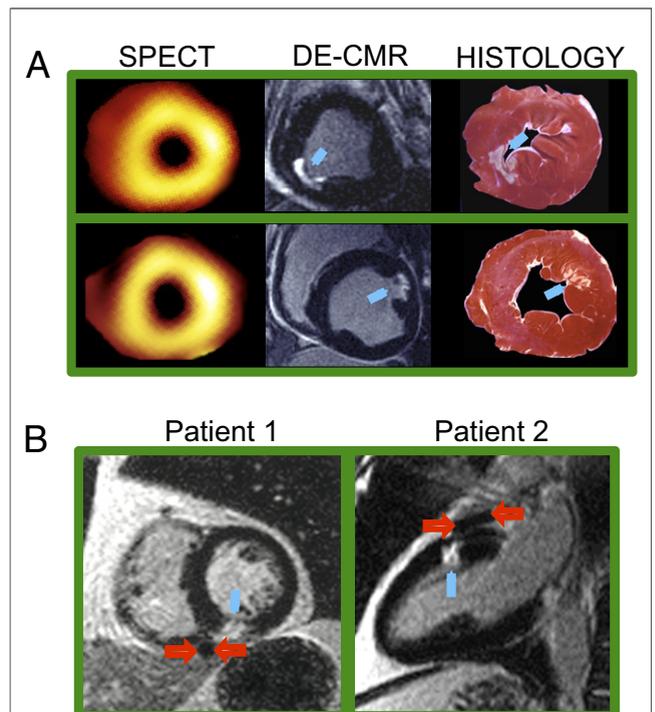
Figure 2 **MI Visualized by DE-CMR**

(A) Comparison of delayed-enhancement (DE)-CMR with histopathology and single-photon emission computed tomography (SPECT) in 2 animals with subendocardial MI. Note that the size and shape of hyperenhanced regions by DE-CMR **(blue arrows)** match the size and shape of infarcted regions delineated by histological vital staining. No infarcts are evident by SPECT. Modified, with permission, from Wagner et al. (8). **(B)** Microinfarction **(blue arrows)** associated with successful percutaneous coronary intervention is shown in 2 patients. **Red arrows** point to the coronary stents. Modified, with permission, from Ricciardi et al. (9). Guidelines for DE-CMR parameter adjustments may be found elsewhere (14,23–25). Abbreviations as in Figure 1.

Recently, the performance of DE-CMR for the detection of MI was tested in an international multicenter trial (12). In total, 282 patients with acute and 284 with chronic first-time MI were scanned in 26 centers throughout the U.S., Europe, and South America. The study showed that the sensitivity of DE-CMR increased with increasing gadolinium dose, reaching 99% and 94% in acute and chronic MI, respectively, with the 0.3-mmol/kg dose (Fig. 3). Furthermore, with doses 0.2 mmol/kg or higher, when MI was identified, it was in the correct location in more than 97% of patients (i.e., the location of hyperenhancement matched the perfusion territory of the infarct-related artery). Importantly, this study represents the first multicenter trial designed to evaluate an imaging approach for detecting MI. Although several multicenter trials have used infarct size measurements by SPECT as a surrogate end point to assess the efficacy of an investigative therapy (41), these trials were not designed to evaluate SPECT, and limited multicenter data on the sensitivity or accuracy of radionuclide imaging for detecting or localizing MI have been reported. In addition, the multicenter DE-CMR trial tested the sensitivity of imaging for both acute and chronic MI. This is notable because there are far fewer clinical trial data on the detection of chronic MI, and chronic infarcts are generally more difficult to detect than acute infarcts because substantial shrinkage can occur during healing (7). Thus, in sum, the data indicate that DE-CMR is a well-validated, robust technique that can be easily implemented on scanners that are commonly available worldwide, with an effectiveness that rivals the best available imaging techniques for the detection and assessment of MI.

Diagnosis and Assessment of MI

Issues in clinical diagnosis. According to the American College of Cardiology/European Society of Cardiology consensus document on the universal definition of MI, the cornerstone tests for the diagnosis are troponins and the electrocardiogram (ECG) (6). Unfortunately, these tests have some limitations. Although troponin assays are exquisitely sensitive and can detect minute amounts of myocardial necrosis, levels are elevated for only a few days after an acute event (42). Importantly, many patients do not have classic symptoms and do not seek medical attention within the time window when troponins are elevated. The consequence is that many subacute and all chronic infarcts will not be identified by troponins. The ECG is helpful in this situation, and incident Q waves have been the basis for diagnosing silent or clinically unrecognized MI in population studies (43). These surveys have shown that unrecognized MIs are common, comprising as many as 40% to 60% of all MIs. By definition, however, all unrecognized infarcts that are non–Q-wave will be missed (44). Additionally, Q waves often occur in the setting of nonischemic cardiomyopathy, and the specificity of the ECG may be poor in the setting of other cardiopulmonary disorders (45).

In these circumstances, cardiac imaging has the potential to provide corroborative diagnostic information. The universal definition indicates that new regional wall motion abnormalities or a loss of viable myocardium could be considered evidence of MI (6). However, wall motion abnormalities may not occur unless the infarcted region exceeds 20% to 50% of the myocardial wall (2,46). Similarly, scintigraphic defects may not be apparent until >10 g of tissue is infarcted (2). Thus, because a sizable threshold of damage is required, echocardiography or SPECT may miss MI, particularly when it is small or subendocardial. Conversely, when abnormalities in regional function or perfusion are present, they do not always indicate MI. Both may be abnormal in the setting of ischemia without infarction. Nonischemic conditions, such as cardiomyopathy or inflammatory or infiltrative diseases, can also lead to wall motion abnormalities or loss of viable myocardium. Hence, the

SENSITIVITY (%)

Acute MI (n=282)

Pre-Contrast: 14 (6-22), 13 (5-21), 17 (8-26), 15 (7-24)
Post-10 Mins: 48 (36-59), 84 (76-93), 95 (90-100), 99 (97-100)
Post-30 Mins: 45 (34-56), 80 (70-89), 92 (86-98), 99 (98-100)

Chronic MI (n=284)

Legend — Dose (mmol/kg) Gadoversetamide: 0.05, 0.1, 0.2, 0.3

Pre-Contrast: 6 (1-12), 3 (0-7), 8 (2-15), 10 (3-17)
Post-10 Mins: 52 (40-63), 83 (74-91), 87 (79-95), 94 (89-100)
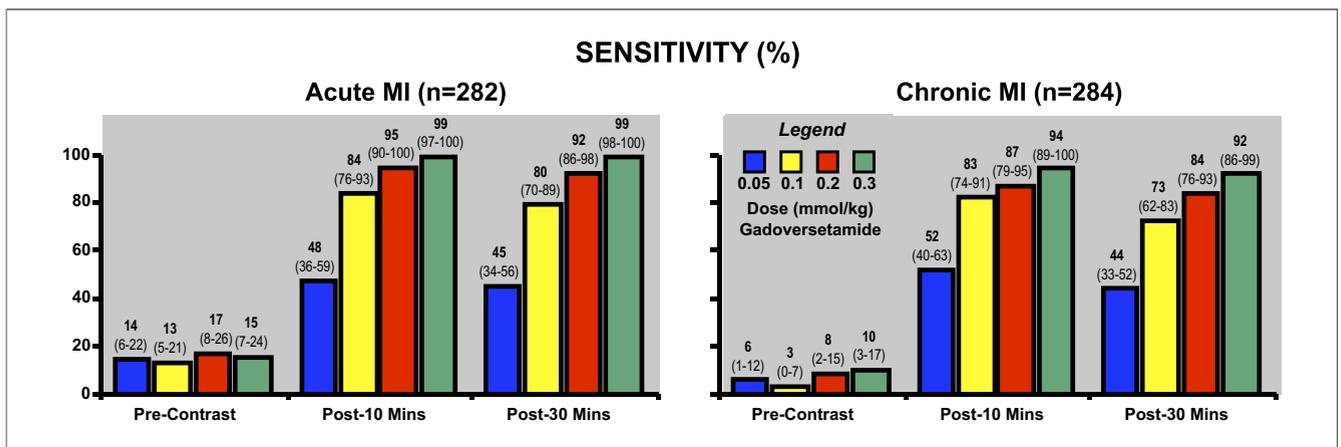Post-30 Mins: 44 (33-52), 73 (62-83), 84 (76-93), 92 (86-99)

Figure 3   Sensitivity of DE-CMR for Acute and Chronic MI

The diagnostic sensitivity of detecting MI is summarized according to gadoversetamide dose group and imaging time point.
Numbers in parentheses are 95% confidence intervals. Modified, with permission, from Kim et al. (12). Abbreviations as in Figures 1 and 2.

positive predictive value of these imaging findings is not high unless these conditions can be excluded (6).

Even some patients who have all of the classic features of MI—for example, chest pain, new ST-segment changes, and an increase in troponins—and fulfill the universal definition, may ultimately prove not to have had an MI. For instance, it is well known that ST-segment changes and elevated troponins can occur in the setting of many disorders, including myocarditis, Takotsubo cardiomyopathy, trauma, pulmonary embolism, and drug toxicity (6). The prevalence of these disorders is poorly characterized, but notably, several studies have shown that a nontrivial proportion of patients with clinically suspected MI have normal coronary arteries or insignificant disease at angiography, including up to 10% of patients initially diagnosed with ST-segment elevation myocardial infarction (STEMI) and 32% with acute coronary syndrome (ACS) (Table 1) (47–62). Although recanalization after an occlusive coronary event is well documented (63,64), many of these patients are unlikely to have had an MI, leaving clinicians with unanswered questions regarding diagnosis and management.

Improving diagnosis. In situations such as these, where the diagnosis of MI by the universal definition is difficult, DE-CMR may prove to be helpful. One emerging application has been the identification of unrecognized MI. Among 195 patients without a history of MI undergoing clinically indicated CMR, Kwong et al. (65) found that the prevalence of unrecognized MI by DE-CMR was 76% higher than by ECG. Among 185 patients with clinically suspected CAD who underwent CMR for research purposes (not clinically ordered), Kim et al. (44) reported that the prevalence of unrecognized MI by DE-CMR was 313% higher than by ECG. In 259 randomly chosen 70-year-old residents of Uppsala, Sweden, Barbier et al. (66) observed a 390% higher rate. In all 3 studies, several patients with Q waves did not have hyperenhancement, which probably reflects the limited specificity of electrocardiography for diagnosing MI.

From a public health standpoint, the implications of these studies may be considerable. It has been estimated that 190,000 patients in the U.S. and perhaps as many as 300,000 in Europe suffer from unrecognized MI annually

Table 1	Prevalence of Nonobstructive CAD in Patients With MI or ACS Undergoing Angiography							
				Nonobstructive CAD				
					Prevalence (%)			
Study	Year	n*	Definition	Overall	M	F	No Single Culprit (None, Multiple)	Ref. #
STEMI								
Larson et al.	2007	1,335	<50%	10	8	14	15% (14%, 1%)	61
DANAMI-2 substudy	2007	516	<50%	4	—	—	—	47
CAPTIM	2002	405	—	10†	—	—	—	48
GUSTO IIb	1999	2,251	—	8	7	10	—	49
NSTEMI								
ICTUS substudy	2007	599	<70%	9	—	—	—	50
CRUSADE	2006	38,301	<50%	9	6	12	—	51
TACTICS–TIMI 18 substudy	2005	542	<50%	6	4	10	—	52
FRISC II substudy	2001	1,142‡	<50%	7	4	14	44%‡	53
GUSTO IIb	1999	1,749	—	5	4	9	—	49
Non–Q-wave MI								
VANQWISH substudy	2002	350	<50%	6	—	—	51% (37%, 14%)	54
NSTEMI and ACS (negative biomarker)			—					
SYNERGY	2007	7,005	—	8	—	—	—	55
Bugiardini et al.	2006	7,656	<50%	9	—	—	—	56
ISAR-COOL	2003	410	<50%	11	—	—	—	57
RITA-3	2002	865	<70%	22	—	—	—	58
PURSUIT	2000	5,767	≤50%	12	—	—	—	59
TIMI IIIB	1994	1,193	≤60%	16	—	—	—	60
STEMI, NSTEMI, and ACS (negative biomarker)								
GRACE	2009	26,755	<50%	8	6	12	—	61
MATE	1998	163	<70%	25	—	—	45% (44%, 1%)	62
ACS (negative biomarker)								
TACTICS–TIMI 18 substudy	2005	353	<50%	21	17	28	—	52
FRISC II substudy	2001	1,142‡	<50%	32	26	43	44%‡	53
GUSTO IIb	1999	2,406	—	20	14	31	—	49

*Patients who underwent angiography and had data available. †Estimated from patients in angioplasty arm not undergoing percutaneous coronary intervention because of normal coronary flow or no explanation provided. ‡Values reflect the data from the combined group of NSTEMI and ACS with negative biomarker.
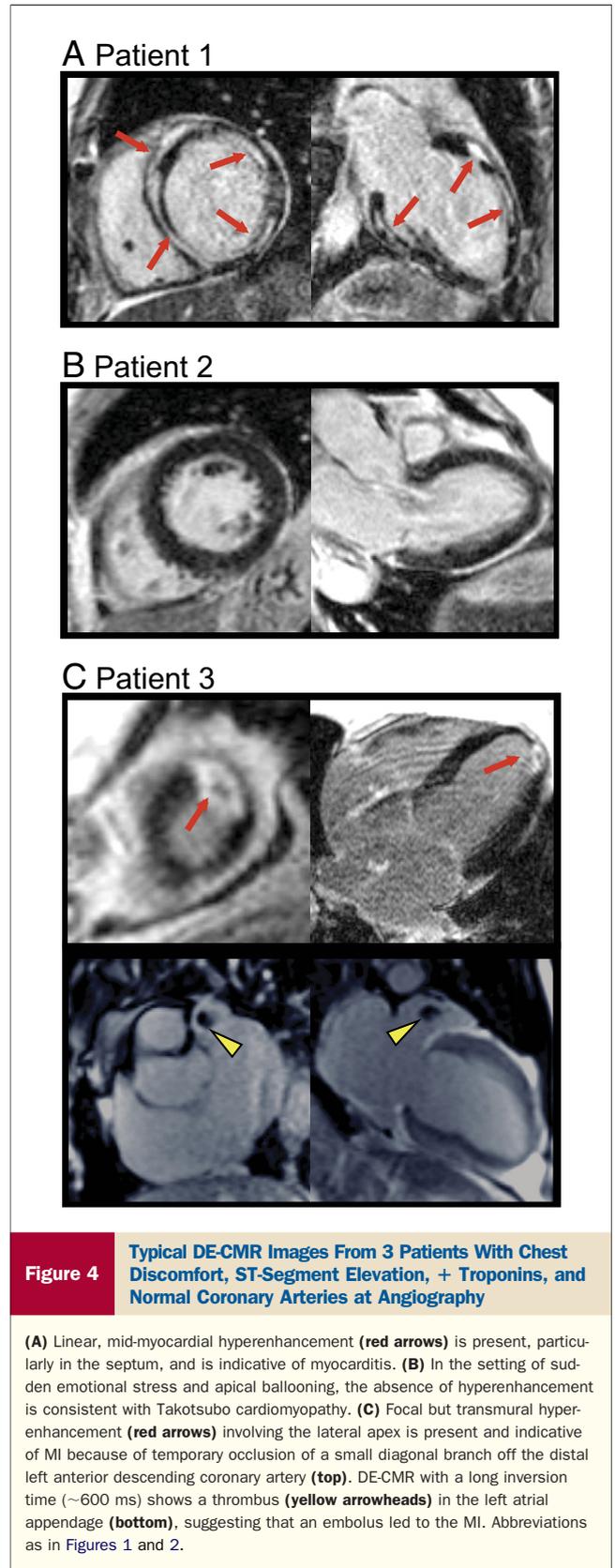
— = data not available; ACS = acute coronary syndrome; CAD = coronary artery disease; F = female; M = male; MI = myocardial infarction; NSTEMI = non–ST-segment elevation myocardial infarction; STEMI = ST-segment elevation myocardial infarction.

(67,68). Because these estimates reflect only patients identified by ECG, the DE-CMR studies suggest that the actual incidence may be 3-fold higher. However, infarct size is larger and left ventricular ejection fraction (LVEF) is lower in patients with unrecognized MI with Q waves than those without (44), and one might question whether the prognosis of individuals with unrecognized MI by DE-CMR is relatively benign. On this point, we note that Kwong et al. (65) reported that the presence of unrecognized MI by DE-CMR conferred nearly a 6-fold increased risk for major adverse cardiac events. Likewise, Kim et al. (44) reported that the presence of unrecognized non–Q-wave MI predicted an 11-fold higher risk of all-cause mortality than those without MI.

Initial studies suggest that CMR may also be useful in the emergency department setting for the evaluation of patients with chest pain. Kwong et al. (69) showed that a multitechnique CMR examination can be performed rapidly and safely in emergency department patients, and reported that CMR added diagnostic value over standard clinical assessment for the diagnosis of ACS. Cury et al. (70) reported similar findings, but also showed that CMR has the potential to diagnose acute MI even when the first troponin measurement is negative.

Similar to troponins, the detection of injury by DE-CMR is specific for irreversible myocardial damage but is not specific for MI. One potential advantage of DE-CMR is that the pattern of hyperenhancement, rather than simply the presence or extent, may offer important information regarding the etiology of myocardial damage (71–73). For this purpose, the concept that ischemic myonecrosis proceeds as a wavefront (74) from the subendocardium to the epicardium with increasing coronary occlusion time is crucial. Correspondingly, hyperenhancement patterns that spare the subendocardium and are limited to the middle or epicardial portion of the left ventricular (LV) wall are invariably nonischemic in origin because damage in the setting of CAD almost always involves the subendocardium (71–73). Moreover, certain nonischemic disorders, such as myocarditis, have characteristic hyperenhancement patterns that suggest specific diagnoses, and a systematic approach to interpreting DE-CMR images in patients with cardiomyopathy has been proposed (72,75). Figure 4 shows representative examples of how DE-CMR may be clinically useful in 3 patients presenting with chest discomfort, ST-segment elevation, and positive troponins. In all 3, the initial diagnosis was STEMI, but insignificant CAD was found at coronary angiography. DE-CMR was performed because the diagnosis was uncertain, and in each case provided information to clarify the diagnosis.

Data regarding the prevalence of the heterogeneous disorders that may mimic MI are limited. However, recently, Assomull et al. (76) evaluated the role of CMR in 60 patients presenting with chest pain, elevated troponins, and unobstructed coronary arteries. DE-CMR provided a new diagnosis in 65% of patients (myocarditis was most com-

Figure 4   **Typical DE-CMR Images From 3 Patients With Chest Discomfort, ST-Segment Elevation, + Troponins, and Normal Coronary Arteries at Angiography**

(A) Linear, mid-myocardial hyperenhancement **(red arrows)** is present, particularly in the septum, and is indicative of myocarditis. **(B)** In the setting of sudden emotional stress and apical ballooning, the absence of hyperenhancement is consistent with Takotsubo cardiomyopathy. **(C)** Focal but transmural hyperenhancement **(red arrows)** involving the lateral apex is present and indicative of MI because of temporary occlusion of a small diagonal branch off the distal left anterior descending coronary artery **(top)**. DE-CMR with a long inversion time (~600 ms) shows a thrombus **(yellow arrowheads)** in the left atrial appendage **(bottom)**, suggesting that an embolus led to the MI. Abbreviations as in Figures 1 and 2.

mon) and excluded significant pathology in the remainder. In a registry of 1,335 STEMI patients undergoing coronary angiography, Larson et al. (77) reported that 14% had no

culprit artery and 9.5% did not have significant CAD. In the group without a clear culprit artery, CMR established that the most common diagnoses were myocarditis (31%), Takotsubo cardiomyopathy (31%), and STEMI without an angiographic lesion (29%). Concerning the latter, Table 1 shows that in many patients with acute MI or ACS, the culprit artery cannot be identified because of the absence of CAD or the absence of typical angiographic characteristics, or because multivessel CAD is present and more than 1 artery/culprit could be responsible. In these circumstances, by visualizing the MI location, DE-CMR may be helpful in identifying the infarct-related artery (Fig. 4C).

Improving infarct characterization and identification of sequelae. Even when the diagnosis of MI is certain, it is often useful to further characterize the infarct and identify sequelae. Infarct size can be measured accurately and with a high level of reproducibility in both acute and chronic settings (32,78,79). Additionally, the high spatial resolution of DE-CMR allows determination of the transmural extent of infarction, which provides supplemental information to infarct size in predicting improvement in contractile function with mechanical revascularization or medical therapy (35,80–83). DE-CMR may also allow assessment of gradations of injury within acute MI. Rather than simply identifying a region of acute infarction as nonviable, DE-CMR can distinguish acute infarcts with only necrotic myocytes from acute infarcts with necrotic myocytes and damaged microvasculature (Fig. 5A). The latter is associated with more severe ischemic injury and results in compromised tissue perfusion even after restoration of epicardial coronary flow. Microvascular damage, also known as the no-reflow phenomenon, is important to detect because it appears to be associated with adverse ventricular remodeling and poor clinical outcome (84–87).

Increasing experience with CMR has led to the development of new applications that may be used to diagnose adverse sequelae associated with MI, including right ventricular involvement, acute pericarditis, and LV thrombus
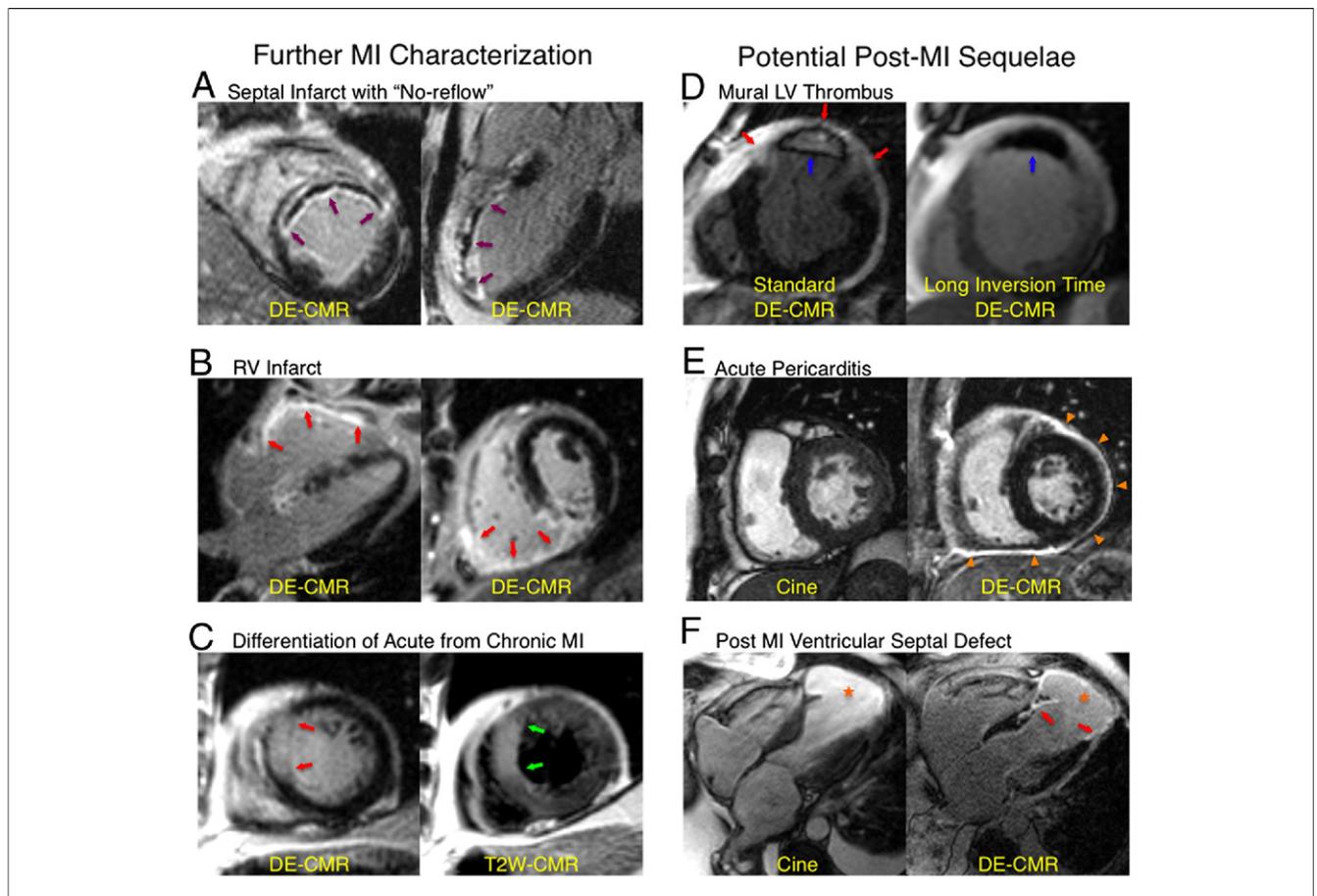

Figure 5   MI Characterization and Potential Post-MI Sequelae

Examples are shown of patients with MI complicated by the presence of **(A)** microvascular damage (no reflow, **purple arrows**), and **(B)** right ventricular (RV) involvement **(red arrows)**. **(C)** Acute infarcts **(red arrows)** can be differentiated from chronic infarcts by the use of T2-weighted imaging, which can show increased signal in areas of acute necrosis **(green arrows)**. **(D)** Post-MI sequelae such as mural thrombus **(blue arrows)** can be identified by DE-CMR. Long-inversion-time imaging may improve detection because the image intensity of viable myocardium is gray rather than black. Thrombus is often immediately adjacent to infarcted myocardium **(red arrows)**. **(E)** Acute pericarditis can be diagnosed by the presence of hyperenhanced pericardium **(orange arrowheads)**. **(F)** CMR image may be used to define ventricular septal defect location **(orange stars)**, extent of associated infarction **(red arrows)**, and severity of shunting. T2W = T-2 weighted; other abbreviations as in Figure 2.

(Figs. 5B to 5F). In patients with acute inferior MI, Kumar et al. (88) showed that even when physical examination, ECG with right precordial leads, and echocardiography were negative, DE-CMR could detect right ventricular involvement in nearly 25% of patients. Taylor et al. (89) used a multitechnique CMR examination to evaluate patients with pericardial disease. Pericardial hyperenhancement appeared to be both sensitive and specific for inflammatory pericarditis, as verified by histopathology, whereas pericardial thickening without hyperenhancement was consistent with a noninflammatory fibrotic pericardium. In patients with MI or ischemic cardiomyopathy, Mollet et al. (90) reported that DE-CMR identified LV thrombus in substantially more patients than cine-CMR or transthoracic echocardiography; however, a reference standard was not available. Srichai et al. (91) evaluated a protocol combining cine- and DE-CMR for the diagnosis of LV thrombus in patients with advanced ischemic cardiomyopathy undergoing surgical LV reconstruction. Among 160 patients (in whom there was surgical and/or pathological confirmation of thrombus), CMR showed higher sensitivity and specificity (88% and 99%, respectively) than transthoracic (23%, 96%) and transesophageal (40%, 96%) echocardiography. Weinsaft et al. (92) assessed the prevalence of LV thrombus by cine and DE-CMR in 784 consecutive patients with systolic dysfunction. The DE-CMR detected a higher prevalence than cine-CMR (7.0% vs. 4.7%, p < 0.005), and follow-up for embolic events or pathological confirmation was consistent with DE-CMR as the better reference standard. Interestingly, patients with ischemic cardiomyopathy were 5 times more likely to have thrombus than those with nonischemic cardiomyopathy despite similar LVEF. Additionally, myocardial scarring by DE-CMR was identified as a novel risk factor for thrombus.

The ability of DE-CMR to identify thrombus based on tissue characteristics rather than just anatomical appearance likely explains its improved performance compared with cine-CMR or noncontrast echocardiography. The basic underlying principle is that thrombi are avascular and have essentially no gadolinium uptake. Thus, thrombus can be identified as a nonenhancing defect surrounded by bright ventricular blood and contrast-enhanced myocardium. Image intensity differences between normal myocardium and thrombus can be accentuated by using a DE-CMR sequence in which the inversion time is increased to null avascular tissue such as thrombus (500 to 600 ms) (92). With long-inversion-time imaging, regions with contrast uptake such as viable myocardium increase in image intensity, whereas thrombus appears homogeneously black, and there is improved delineation, particularly of mural thrombus (Fig. 5D). The concept that contrast uptake, albeit low, is not zero in normal myocardium, is one reason why we prefer to describe nonviable regions as hyperenhanced rather than simply enhanced because depending on the DE-CMR settings, viable myocardium can show contrast enhancement compared with avascular tissue.

Figure 6 outlines possible CMR findings in patients with suspected MI. Furthermore, it shows the potential of CMR to provide additive diagnostic information and how CMR may be incorporated with traditional clinical assessment.

CMR Infarct Size as a Surrogate End Point for Clinical Trials

The ultimate goal of a new therapy for acute MI is a reduction in mortality. In the current era, treatment of acute MI is quite effective; therefore, demonstrating a further reduction in mortality with novel treatments is increasingly difficult and necessitates studies with large sample sizes. This requirement imposes significant logistical and financial barriers on testing potential new therapies, and correspondingly limits the number of treatments that can be evaluated. As such, there is considerable interest in using surrogate end points to assess the efficacy of acute MI therapies. Infarct size is a particularly attractive surrogate end point for several reasons (41,93). First, it is useful in early screening studies to test whether a new therapy is biologically active. Second, it can serve as an end point for phase II dose-ranging studies to test efficacy and/or safety. Third, it may indicate a late mortality benefit, and thus rationale for performing a longer-term study, even if an early benefit is not seen. For instance, a reduction in infarct size may lead to a long-term improvement in ventricular remodeling, a benefit that may not be manifest on 30-day mortality rates. Fourth, it can provide a mechanism for improvement in outcome, because prognosis after acute MI is strongly determined by infarct size (94,95). Several investigations have reported that infarct size measured by DE-CMR is a stronger predictor of outcome than LVEF and LV volumes (96–98).

When to measure infarct size. Measurements of infarct size in the first few weeks after infarction need to take into account what Reimer and Jennings (74) termed the changing anatomic reference base of evolving myocardial infarction. In their pioneering studies, they showed that infarct volume can almost double during the first few days after coronary artery occlusion, even in the absence of additional myocyte death via lethal reperfusion injury or infarct extension, because of the addition of edema and cellular elements. In contrast, infarct volume may shrink to 25% of its initial volume as necrotic muscle is replaced by scar over 4 to 6 weeks.

Using DE-CMR, similar findings have been observed in vivo in a canine model (Fig. 7) (99,100). Fieno et al. (99) showed that terminal infarct size at 4 to 8 weeks averaged 24% of that found at 3 days, and reperfusion accelerated infarct resorption. Moreover, the mass of viable myocardium increased systematically with time, although the time course of hypertrophy was different from that of infarct resorption. Importantly, measurements of total LV mass did not reflect the changes occurring separately in infarcted and viable regions. These results highlight the capability of DE-CMR to improve the assessment of post-infarction
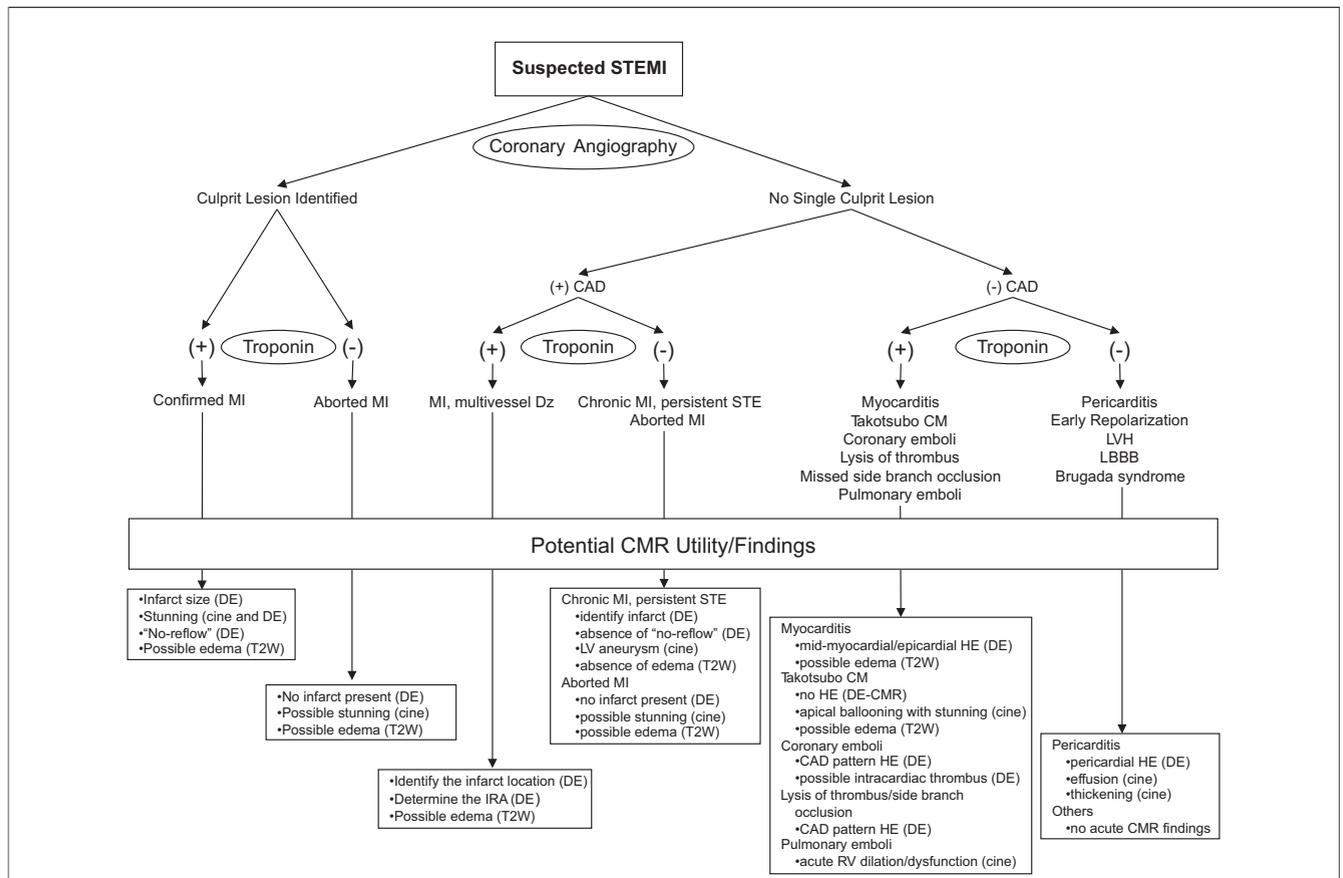
Figure 6   **Schema Highlighting the Potential Utility of CMR in Patients With Suspected STEMI**

Suspected STEMI patients often undergo early coronary angiography. When a culprit lesion is identified with an appropriate increase in troponins, then MI is confirmed. An isolated, partially recanalized lesion without subsequent troponin elevation indicates an aborted MI. In this situation, CMR will not show an MI, but myocardial stunning and/or edema may be seen. If diffuse multivessel disease is seen along with multiple potential culprit lesions and troponins are elevated, CMR may help identify the infarct-related artery by showing the location of acute necrosis and associated edema. If CAD is present but a culprit lesion is not identified and troponins are not elevated, the presence of a chronic MI by CMR indicates the diagnosis of chronic MI with persistent ST-segment elevation. If CMR does not detect MI but stunning and/or edema is present, an aborted MI is suggested. Troponin elevation in the apparent absence of CAD may occur in a number of settings, including myocarditis, Takotsubo cardiomyopathy, coronary emboli, lysis of thrombus, missed ostial side branch occlusion, or pulmonary embolism. Various CMR findings may point to a specific diagnosis. If CAD is absent and troponins are not elevated, CMR may be helpful in identifying pericardial pathology or ruling out acute cardiac pathology. CAD = coronary artery disease; CM = cardiomyopathy; Dz = disease; HE = hyperenhancement; IRA = infarct-related artery; LBBB = left bundle branch block; LVH = left ventricular hypertrophy; RV = right ventricular; STE = ST-segment elevation; STEMI = ST-segment elevation myocardial infarction; T2W = T2-weighted; other abbreviations as in Figures 1 and 2.
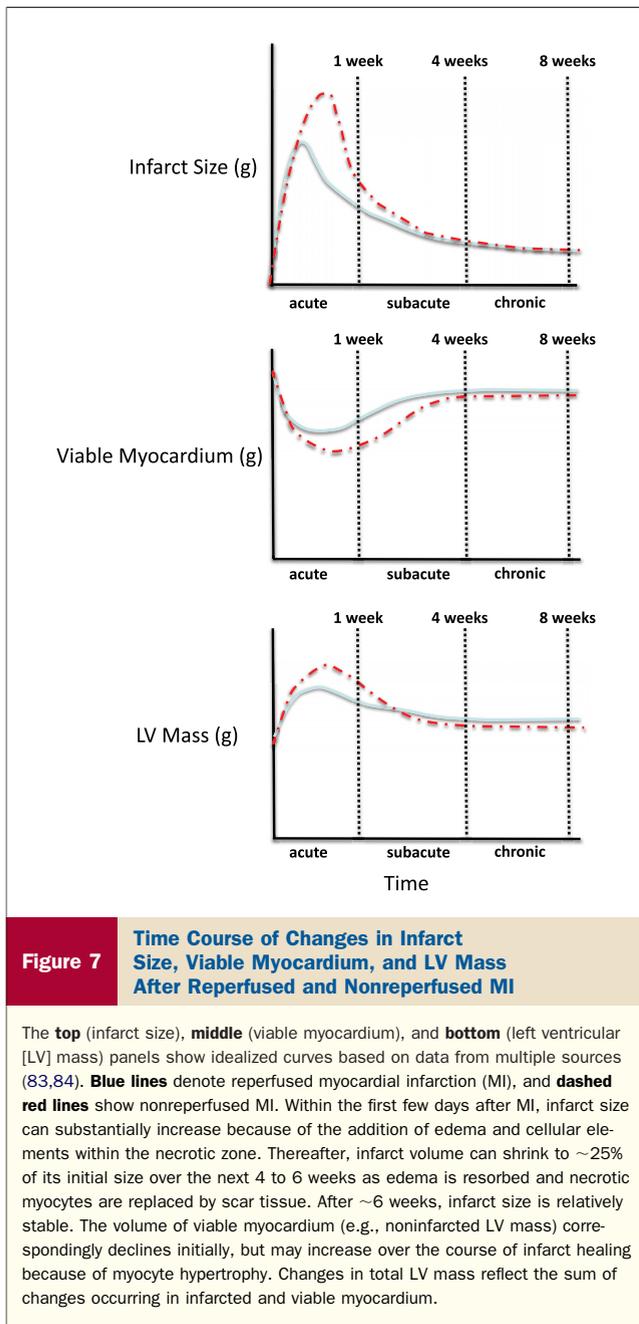
ventricular remodeling by allowing evaluation of concurrent changes such as resorption of infarcted tissue and hypertrophy of viable myocardium at an early time point before measurements of ventricular volumes and mass have changed.

Thus, given the changing anatomic reference base, it is critical to define the timing of infarct size measurement after MI. There are both advantages and disadvantages of measuring infarct size early versus late after MI, and these are listed in Table 2. For any particular study, the chosen time point will depend on the question being addressed and the logistics of the trial.

How to measure infarct size on DE-CMR image. Several methods have been used for the measurement of DE-CMR infarct size. The simplest of these is visual assessment. Hyperenhancement is scored on a 17-segment model with a 5-point scale for each segment (0 = no hyperenhancement,

1 = 1% to 25%, 2 = 26% to 50%, 3 = 51% to 75%, 4 = 76% to 100%) (16,81). Dark regions entirely encompassed within hyperenhanced myocardium are interpreted as regions of microvascular damage (no-reflow) and included as part of the infarct. Infarct size as percent LV myocardium is calculated by summing the regional scores, each weighted by the hyperenhancement range midpoint (i.e., 1 = 13%, 2 = 38%, 3 = 63%, 4 = 88%) and dividing by 17 (12,16). This system allows for rapid assessment of infarct size in increments of ~1.2% of LV mass. Alternatively, infarct size can be quantified by planimetry of hyperenhanced areas on the stack of short-axis images.

In an attempt to be more objective, several semiautomatic methods have been proposed. Initial studies showed that a simple image intensity threshold of 2 to 3 SD above the mean of remote, normal myocardial intensity resulted in infarct size measurements that were nearly identical to that

Figure 7   Time Course of Changes in Infarct Size, Viable Myocardium, and LV Mass After Reperfused and Nonreperfused MI

The **top** (infarct size), **middle** (viable myocardium), and **bottom** (left ventricular [LV] mass) panels show idealized curves based on data from multiple sources (83,84). **Blue lines** denote reperfused myocardial infarction (MI), and **dashed red lines** show nonreperfused MI. Within the first few days after MI, infarct size can substantially increase because of the addition of edema and cellular elements within the necrotic zone. Thereafter, infarct volume can shrink to ~25% of its initial size over the next 4 to 6 weeks as edema is resorbed and necrotic myocytes are replaced by scar tissue. After ~6 weeks, infarct size is relatively stable. The volume of viable myocardium (e.g., noninfarcted LV mass) correspondingly declines initially, but may increase over the course of infarct healing because of myocyte hypertrophy. Changes in total LV mass reflect the sum of changes occurring in infarcted and viable myocardium.

that uses a threshold value of 50% of the maximum intensity within the infarct (full-width at half-maximum [FWHM]) may be more resistant to surface-coil intensity variations and provide improved reproducibility (31). Unfortunately, FWHM assumes a bright infarct core, and may not be accurate if the infarct is homogeneously gray (Fig. 8). Additionally, FWHM may be troublesome if there are multiple infarcts and/or the infarct is patchy with multiple, separate islands of necrosis. More sophisticated algorithms have been proposed that assign a weighting to each voxel depending on its image intensity (102) or use a combination of methods along with regional feature analysis (103,104). Although promising, these newer methods (and many semiautomated methods) are not widely available, have been tested in few patients, and have not been shown to work equivalently for images from different magnetic resonance imaging vendors. The latter would be important for multicenter trials.

Moreover, these semiautomated methods are not as objective as one might think. All require user input to distinguish bright artifact and/or noise voxels (false-positive regions) and dark no-reflow voxels (false-negative regions). Most important, all require manual tracing of the myocardial borders. This is because there are no automated algorithms that can reliably distinguish the bright LV cavity from the bright endocardial border of the infarct. Indeed, tissue contrast-to-noise ratio is far lower between infarct and LV cavity than between infarct and normal myocardium (16,105). Because the endocardial border may constitute up to 50% of the infarct perimeter, this portion of the infarct border may be the largest source of variability in infarct size measurements. Given these issues, we prefer to planimeter the infarct visually in our core laboratory using experienced readers who can carefully segment myocardial borders and can account for artifacts, no-reflow regions, and areas with intermediate image intensity. Several laboratories have shown low intraobserver and interobserver variability in quantifying infarct size visually using experienced readers (44,79,101,106).

Sample size considerations. When testing new therapies using infarct size as a surrogate end point, sample size (*n*) calculations are based on the following formula:

$$n = \frac{2(\sigma^2)(z_{\alpha/2} + z_\beta)^2}{\delta^2}$$

where σ is the standard deviation of infarct size, δ is the expected reduction in infarct size due to the new therapy, and z is the value of the z-statistic depending on the alpha and beta levels set by the study design. Thus, sample size is determined by both the expected effect of the therapy (δ) and the variability of measured infarct size within a population (σ) (107). The latter is comprised of 2 components: the variability in infarct size between patients (σ_T) and the reproducibility (σ_e) of the sizing method (e.g., standard error of the measurement).

provided by histopathology (7,29). However, these were experimental studies that validated high-resolution (0.5 × 0.5 × 0.5 mm) ex vivo imaging. For imaging in vivo, spatial resolution is over 100 times worse, cardiac motion can lead to further blurring, and partial-volume effects can result in voxels with intermediate image intensity (7). In this situation, using a 2- to 3-SD threshold may lead to overestimation of infarct size because gray zones, which represent an admixture of viable and nonviable myocytes, are incorrectly categorized as fully bright and thus 100% infarcted (101). Although a higher cutoff could reduce overestimation, this method is highly dependent on the choice of the remote zone used to calculate the threshold. An alternative method

Table 2	Measurement of Infarct Size: Early Versus Late	
	Early (≤7 to 10 Days)	Late (>4 Weeks)
Advantages		
	Larger infarct size	Infarct size is stable
	Higher detection rate	Imaging time frame can be wide
	May reduce required sample size	Can also assess LVEF, which is stable (stunning, if present, has resolved)
	Can also assess presence and extent of no reflow	Can also assess recovery of function
	Can also assess presence and extent of stunning	Can also assess early ventricular remodeling
Disadvantages		
	Infarct size is dynamic	Presumes survival and successful follow-up
	Imaging time frame must be narrow (≤3 days)	Smaller infarct size
	Requires patient stability	May increase required sample size
		Infarct healing (shrinkage) may preclude detection of very small MI

LVEF = left ventricular ejection fraction; MI = myocardial infarction.

Several studies have now been published that show that the measurement of infarct size by DE-CMR is highly reproducible (32,78,79,106). For example, in a 3-center study of patients with acute MI undergoing paired DE-CMR scans, the SD (e.g., σ_e) in repeated measurements was only 1% of LV mass (32). The implication of improved reproducibility is that DE-CMR enables the systematic detection of smaller changes in infarct size, and potentially allows substantial reduction in sample size for clinical trials. However, it has been suggested that this presumes that paired imaging is performed to detect a change in infarct size over time, in which the variability in infarct size between patients (σ_T) is eliminated (41). Unfortunately, paired testing is not feasible in most acute MI trials, and
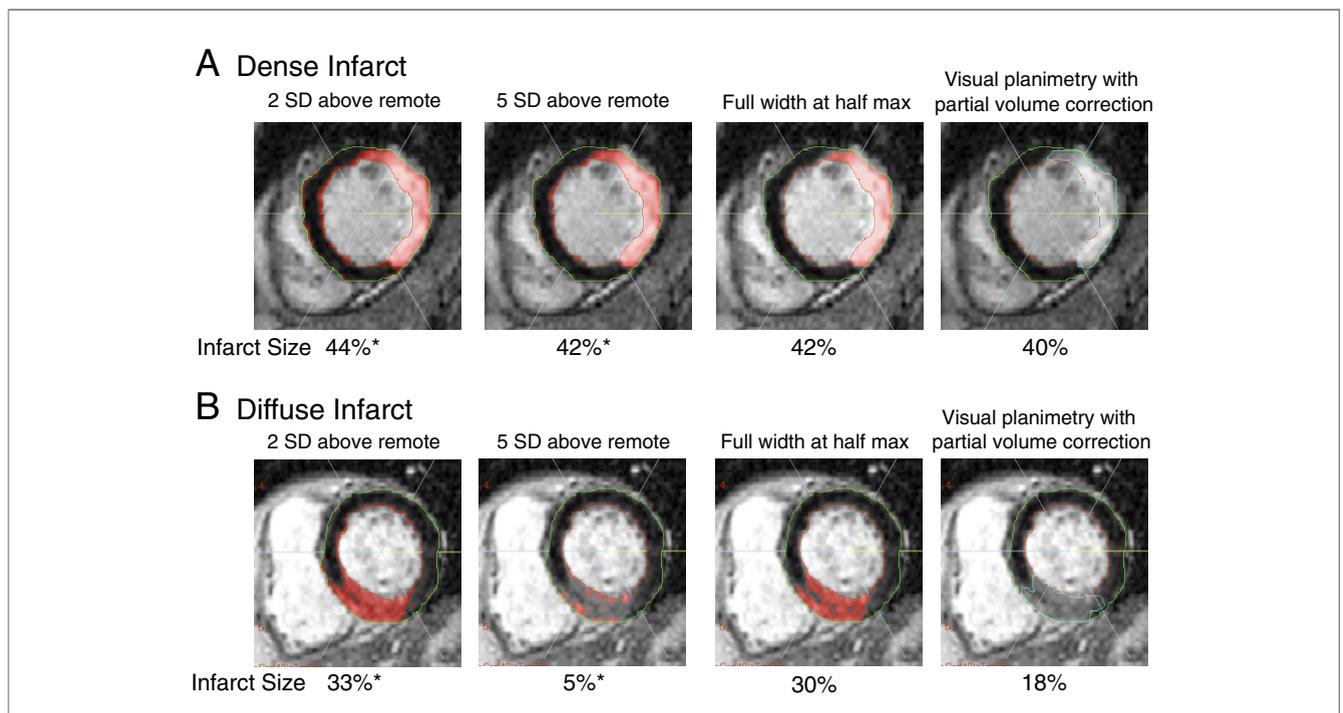

Figure 8   Comparison of Methods for the Quantification of Infarct Size

Examples are shown when infarct size is quantified using 4 different methods when **(A)** the infarct is dense, and **(B)** the infarct is diffuse. Currently, all methods require a user to manually contour epicardial and endocardial contours. Note that when the infarct is dense and image intensity is homogeneously bright, the various methods result in infarct size measurements that are quite similar. When the infarct is diffuse and image intensity is homogeneously gray, using a simple threshold of 2 SD above remote often results in overestimation of infarct size because the entire area that is gray is incorrectly assumed to be 100% infarcted. Higher thresholds may underestimate infarct size if gray zones are incorrectly assumed to be 100% viable. The full width at half maximum (FWHM) method quantifies infarct size by measuring all pixels above a threshold value of 50% of the maximum intensity within the infarct. If the infarct is diffuse and there is no dense core, FWHM can also overestimate infarct size. We prefer to planimeter the infarct visually, but will correct for partial volume effects by accounting for voxels with intermediate image intensity. Partial volume analysis methods weight each voxel within the infarct based on the highest signal intensity within the infarct or the blood cavity (whichever is greater). *Infarct size after user input to remove noise pixels that are beyond the chosen cutoff but are obviously not within the infarcted region.
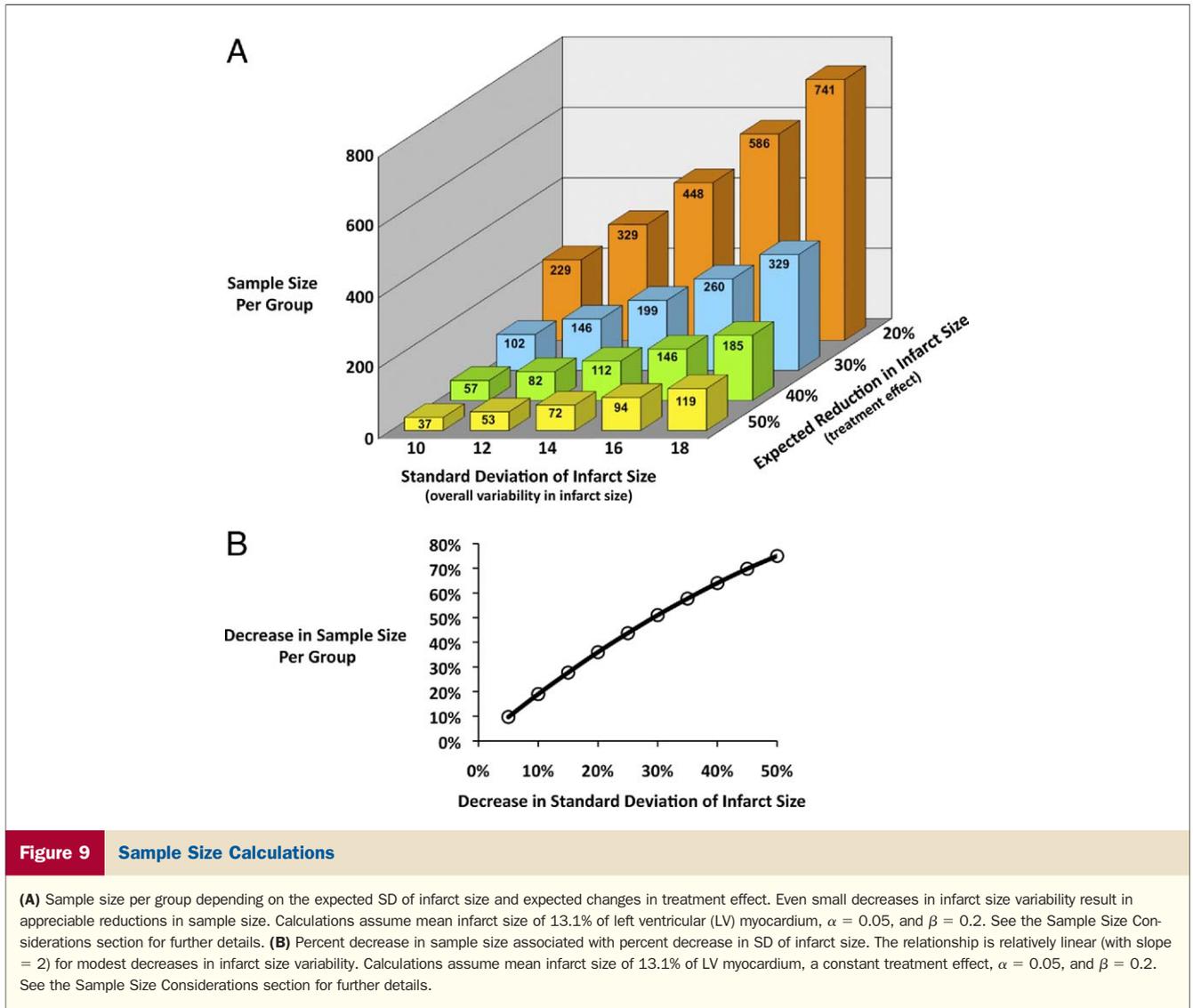
Figure 9   Sample Size Calculations

(A) Sample size per group depending on the expected SD of infarct size and expected changes in treatment effect. Even small decreases in infarct size variability result in appreciable reductions in sample size. Calculations assume mean infarct size of 13.1% of left ventricular (LV) myocardium, $\alpha = 0.05$, and $\beta = 0.2$. See the Sample Size Considerations section for further details. **(B)** Percent decrease in sample size associated with percent decrease in SD of infarct size. The relationship is relatively linear (with slope = 2) for modest decreases in infarct size variability. Calculations assume mean infarct size of 13.1% of LV myocardium, a constant treatment effect, $\alpha = 0.05$, and $\beta = 0.2$. See the Sample Size Considerations section for further details.

infarct size is only assessed after the treatment being tested has been given (unpaired). Thus, because the variability in true infarct size among patients is typically larger than the variability added by the infarct sizing method (e.g., $\sigma_T > \sigma_e$), it is possible that the improved reproducibility of DE-CMR may not translate into significant reductions in sample size (41).

To examine this issue further, Figure 9A illustrates the effect on sample size by changing either the overall variability in infarct size, the treatment effect, or both, given typical values for constants. These calculations show that, for a given treatment effect, even a small decrease in the SD of infarct size, such as 2% of LV mass, would result in a 20% to 30% reduction in sample size for each treatment arm. Figure 9B relates percent changes in the SD of infarct size to percent changes in sample size. For relatively modest decreases in infarct size variability, the plot shows a nearly 2-to-1 linear decrease in sample size. For instance, a decrease in variability by 10% results in a 19% reduction in sample size.

Very few studies have directly compared infarct size measurements by DE-CMR to that by technetium-99m SPECT, although the latter is considered one of the best available techniques for the quantification of infarct size (41). Mahrholdt et al. (78) reported that the SD of infarct size was 6% by DE-CMR and 7.5% by SPECT in a population with chronic MI. Because DE-CMR led to a 20% reduction in variability (1.5 of 7.5), this would result in nearly a 40% reduction in sample size. Similarly, in patients with acute MI, Ibrahim et al. (108) observed that the SD of infarct size by DE-CMR was 13% lower than SPECT (13 vs. 15, respectively). Lunde et al. (109) evaluated infarct size in STEMI patients randomized to intracoronary injection of mononuclear bone marrow cells at both acute and chronic time points. In the control group, both early and late after MI, the SD of infarct size was lower by DE-CMR than by SPECT (14.0 vs. 21.1 and 12.5 vs. 20.9, respectively). Although the variability of infarct size will change with the population being studied (e.g., cohorts with a high prevalence of anterior MI will have larger mean infarct

size and larger SD), these data suggest that total variability is smaller when utilizing DE-CMR and will lead to appreciable differences in sample size. As a result, interest in DE-CMR for infarct size quantification is rapidly growing. When the ClinicalTrials.gov registry is searched using the term "infarct size," a total of 110 studies are listed. Of these, 47 do not involve acute MI (e.g., cerebral infarction) or do not explicitly detail the methodology of measuring infarct size. Of the remaining 63 studies, 38 (60%) have incorporated DE-CMR as an end point (110). Additionally, several randomized trials using infarct size by DE-CMR as a surrogate end point have been recently published (109,111–114).

Summary

In patients with known or suspected MI, CMR provides a comprehensive, multifaceted view of the heart. The data, including those from a recent multicenter clinical trial, indicate that DE-CMR is a well-validated, robust technique that can be easily implemented on scanners that are commonly available worldwide, with an effectiveness that rivals the best available imaging techniques for the detection and assessment of acute and chronic MI. A DE-CMR may be especially useful when patients present outside the diagnostic window of troponins. Moreover, because DE-CMR can uniquely differentiate between ischemic and various nonischemic forms of injury, it may be helpful in cases of diagnostic uncertainty, such as in patients with classical features of MI in whom coronary angiography does not show a culprit lesion. Even after the diagnosis of MI has been made, CMR can provide clinically relevant information with regard to identification of post-MI sequelae and further infarct characterization. The high accuracy and reproducibility of DE-CMR has led to the increasing use of this technique as the preferred method for quantification of infarct size in many clinical trials.

Reprint requests and correspondence: Dr. Raymond J. Kim, Duke Cardiovascular MRI Center, DUMC 3934, Durham, North Carolina 27710. E-mail: raymond.kim@duke.edu.

REFERENCES

1. Yusuf S, Hawken S, Ounpuu S, et al. Effect of potentially modifiable risk factors associated with myocardial infarction in 52 countries (the INTERHEART study): case-control study. Lancet 2004;364:937–52.
2. Alpert JS, Thygesen K, Antman E, et al. Myocardial infarction redefined—a consensus document of The Joint European Society of Cardiology/American College of Cardiology Committee for the redefinition of myocardial infarction. J Am Coll Cardiol 2000;36:959–69.
3. Newby LK, Alpert JS, Ohman EM, et al. Changing the diagnosis of acute myocardial infarction: implications for practice and clinical investigations. Am Heart J 2002;144:957–80.
4. White HD. Things ain't what they used to be: impact of a new definition of myocardial infarction. Am Heart J 2002;144:933–7.
5. Hochholzer W, Buettner HJ, Trenk D, et al. New definition of myocardial infarction: impact on long-term mortality. Am J Med 2008;121:399–405.
6. Thygesen K, Alpert JS, White HD. Universal definition of myocardial infarction. J Am Coll Cardiol 2007;50:2173–95.
7. Kim RJ, Fieno DS, Parrish TB, et al. Relationship of MRI delayed contrast enhancement to irreversible injury, infarct age, and contractile function. Circulation 1999;100:1992–2002.
8. Wagner A, Mahrholdt H, Holly TA, et al. Contrast-enhanced MRI and routine single photon emission computed tomography (SPECT) perfusion imaging for detection of subendocardial myocardial infarcts: an imaging study. Lancet 2003;361:374–9.
9. Ricciardi MJ, Wu E, Davidson CJ, et al. Visualization of discrete microinfarction after percutaneous coronary intervention associated with mild creatine kinase-MB elevation. Circulation 2001;103:2780–3.
10. Selvanayagam JB, Porto I, Channon K, et al. Troponin elevation after percutaneous coronary intervention directly represents the extent of irreversible myocardial injury: insights from cardiovascular magnetic resonance imaging. Circulation 2005;111:1027–32.
11. Ibrahim T, Bulow HP, Hackl T, et al. Diagnostic value of contrast-enhanced magnetic resonance imaging and single-photon emission computed tomography for detection of myocardial necrosis early after acute myocardial infarction. J Am Coll Cardiol 2007;49:208–16.
12. Kim RJ, Albert TS, Wible JH, et al. Performance of delayed-enhancement magnetic resonance imaging with gadoversetamide contrast for the detection and assessment of myocardial infarction: an international, multicenter, double-blinded, randomized trial. Circulation 2008;117:629–37.
13. Shah DJ, Judd RM, Kim RJ. Technology insight: MRI of the myocardium. Nat Clin Pract Cardiovasc Med 2005;2:597–605, quiz 606.
14. Saremi F, Grizzard JD, Kim RJ. Optimizing cardiac MR imaging: practical remedies for artifacts. Radiographics 2008;28:1161–87.
15. Kramer C, Barkhausen J, Flamm S, et al. Standardized cardiovascular magnetic resonance imaging (CMR) protocols, Society for Cardiovascular Magnetic Resonance: Board of Trustees Task Force on Standardized Protocols. J Cardiovasc Magn Reson 2008;10:35.
16. Sievers B, Elliott MD, Hurwitz LM, et al. Rapid detection of myocardial infarction by subsecond, free-breathing delayed contrast-enhancement cardiovascular magnetic resonance. Circulation 2007;115:236–44.
17. Kaji S, Yang PC, Kerr AB, et al. Rapid evaluation of left ventricular volume and mass without breath-holding using real-time interactive cardiac magnetic resonance imaging system. J Am Coll Cardiol 2001;38:527–33.
18. Abdel-Aty H, Zagrosek A, Schulz-Menger J, et al. Delayed enhancement and T2-weighted cardiovascular magnetic resonance imaging differentiate acute from chronic myocardial infarction. Circulation 2004;109:2411–6.
19. Kim WY, Danias PG, Stuber M, et al. Coronary magnetic resonance angiography for the detection of coronary stenoses. N Engl J Med 2001;345:1863–9.
20. Hendel RC, Patel MR, Kramer CM, et al. ACCF/ACR/SCCT/SCMR/ASNC/NASCI/SCAI/SIR 2006 appropriateness criteria for cardiac computed tomography and cardiac magnetic resonance imaging: a report of the American College of Cardiology Foundation Quality Strategic Directions Committee Appropriateness Criteria Working Group, American College of Radiology, Society of Cardiovascular Computed Tomography, Society for Cardiovascular Magnetic Resonance, American Society of Nuclear Cardiology, North American Society for Cardiac Imaging, Society for Cardiovascular Angiography and Interventions, and Society of Interventional Radiology. J Am Coll Cardiol 2006;48:1475–97.
21. Levine GN, Gomes AS, Arai AE, et al. Safety of magnetic resonance imaging in patients with cardiovascular devices: an American Heart Association scientific statement from the Committee on Diagnostic and Interventional Cardiac Catheterization, Council on Clinical Cardiology, and the Council on Cardiovascular Radiology and Intervention: endorsed by the American College of Cardiology Foundation, the North American Society for Cardiac Imaging, and the Society for Cardiovascular Magnetic Resonance. Circulation 2007;116:2878–91.

22. Kribben A, Witzke O, Hillen U, et al. Nephrogenic systemic fibrosis: pathogenesis, diagnosis, and therapy. J Am Coll Cardiol 2009;53: 1621–8.

23. Simonetti OP, Kim RJ, Fieno DS, et al. An improved MR imaging technique for the visualization of myocardial infarction. Radiology 2001;218:215–23.

24. Kim RJ, Shah DJ, Judd RM. How we perform delayed enhancement imaging. J Cardiovasc Magn Reson 2003;5:505–14.

25. Kim RJ, Choi KM, Judd RM. Assessment of myocardial viability by contrast enhancement. In: Higgins CB, Roos AD, editors. Cardiovascular MRI and MRA. Philadelphia, PA: Lippincott, 2003:209–37.

26. Polimeni PI. Extracellular space and ionic distribution in rat ventricle. Am J Physiol 1974;227:676–83.

27. Weinmann HJ, Brasch RC, Press WR, et al. Characteristics of gadolinium-DTPA complex: a potential NMR contrast agent. AJR Am J Roentgenol 1984;142:619–24.

28. Rehwald WG, Fieno DS, Chen EL, et al. Myocardial magnetic resonance imaging contrast agent concentrations after reversible and irreversible ischemic injury. Circulation 2002;105:224–9.

29. Fieno DS, Kim RJ, Chen EL, et al. Contrast-enhanced magnetic resonance imaging of myocardium at risk: distinction between reversible and irreversible injury throughout infarct healing. J Am Coll Cardiol 2000;36:1985–91.

30. Barkhausen J, Ebert W, Debatin JF, et al. Imaging of myocardial infarction: comparison of Magnevist and gadophrin-3 in rabbits. J Am Coll Cardiol 2002;39:1392–8.

31. Amado LC, Gerber BL, Gupta SN, et al. Accurate and objective infarct sizing by contrast-enhanced magnetic resonance imaging in a canine myocardial infarction model. J Am Coll Cardiol 2004;44: 2383–9.

32. Wagner A, Mahrholdt H, Thomson L, et al. Effects of time, dose, and inversion time for acute myocardial infarct size measurements based on magnetic resonance imaging-delayed contrast enhancement. J Am Coll Cardiol 2006;47:2027–33.

33. Saeed M, Weber O, Lee R, et al. Discrimination of myocardial acute and chronic (scar) infarctions on delayed contrast enhanced magnetic resonance imaging with intravascular magnetic resonance contrast media. J Am Coll Cardiol 2006;48:1961–8.

34. Wu E, Judd RM, Vargas JD, et al. Visualisation of presence, location, and transmural extent of healed Q-wave and non-Q-wave myocardial infarction. Lancet 2001;357:21–8.

35. Choi KM, Kim RJ, Gubernikoff G, et al. Transmural extent of acute myocardial infarction predicts long-term improvement in contractile function. Circulation 2001;104:1101–7.

36. Ingkanisorn WP, Rhoads KL, Aletras AH, et al. Gadolinium delayed enhancement cardiovascular magnetic resonance correlates with clinical measures of myocardial infarction. J Am Coll Cardiol 2004;43: 2253–9.

37. Martin TN, Groenning BA, Murray HM, et al. ST-segment deviation analysis of the admission 12-lead electrocardiogram as an aid to early diagnosis of acute myocardial infarction with a cardiac magnetic resonance imaging gold standard. J Am Coll Cardiol 2007;50:1021–8.

38. Giannitsis E, Steen H, Kurz K, et al. Cardiac magnetic resonance imaging study for quantification of infarct size comparing directly serial versus single time-point measurements of cardiac troponin T. J Am Coll Cardiol 2008;51:307–14.

39. Klein C, Nekolla SG, Bengel FM, et al. Assessment of myocardial viability with contrast-enhanced magnetic resonance imaging: comparison with positron emission tomography. Circulation 2002;105: 162–7.

40. Kuhl HP, Beek AM, van der Weerdt AP, et al. Myocardial viability in chronic ischemic heart disease: comparison of contrast-enhanced magnetic resonance imaging with (18)F-fluorodeoxyglucose positron emission tomography. J Am Coll Cardiol 2003;41:1341–8.

41. Gibbons RJ, Valeti US, Araoz PA, et al. The quantification of infarct size. J Am Coll Cardiol 2004;44:1533–42.

42. Katus HA, Remppis A, Neumann FJ, et al. Diagnostic efficiency of troponin T measurements in acute myocardial infarction. Circulation 1991;83:902–12.

43. Kannel WB, Abbott RD. Incidence and prognosis of unrecognized myocardial infarction. An update on the Framingham study. N Engl J Med 1984;311:1144–7.

44. Kim HW, Klem I, Shah DJ, et al. Unrecognized non-Q-wave myocardial infarction: prevalence and prognostic significance in patients with suspected coronary disease. PLoS Med 2009;6:e1000057.

45. Uusitupa M, Pyorala K, Raunio H, et al. Sensitivity and specificity of Minnesota Code Q-QS abnormalities in the diagnosis of myocardial infarction verified at autopsy. Am Heart J 1983;106:753–7.

46. Mahrholdt H, Wagner A, Parker M, et al. Relationship of contractile function to transmural extent of infarction in patients with chronic coronary artery disease. J Am Coll Cardiol 2003;42:505–12.

47. Hofsten DE, Wachtell K, Lund B, et al. Prevalence and prognostic implications of non-sustained ventricular tachycardia in ST-segment elevation myocardial infarction after revascularization with either fibrinolysis or primary angioplasty. Eur Heart J 2007;28:407–14.

48. Bonnefoy E, Lapostolle F, Leizorovicz A, et al. Primary angioplasty versus prehospital fibrinolysis in acute myocardial infarction: a randomised study. Lancet 2002;360:825–9.

49. Hochman JS, Tamis JE, Thompson TD, et al., for the Global Use of Strategies to Open Occluded Coronary Arteries in Acute Coronary Syndromes IIb Investigators. Sex, clinical presentation, and outcome in patients with acute coronary syndromes. N Engl J Med 1999;341: 226–32.

50. Windhausen F, Hirsch A, Sanders GT, et al. N-terminal pro-brain natriuretic peptide for additional risk stratification in patients with non-ST-elevation acute coronary syndrome and an elevated troponin T: an Invasive versus Conservative Treatment in Unstable coronary Syndromes (ICTUS) substudy. Am Heart J 2007;153:485–92.

51. Patel MR, Chen AY, Peterson ED, et al. Prevalence, predictors, and outcomes of patients with non-ST-segment elevation myocardial infarction and insignificant coronary artery disease: results from the Can Rapid risk stratification of Unstable angina patients Suppress ADverse outcomes with Early implementation of the ACC/AHA Guidelines (CRUSADE) initiative. Am Heart J 2006;152:641–7.

52. Dokainish H, Pillai M, Murphy SA, et al. Prognostic implications of elevated troponin in patients with suspected acute coronary syndrome but no critical epicardial coronary disease: a TACTICS-TIMI-18 substudy. J Am Coll Cardiol 2005;45:19–24.

53. Lindahl B, Diderholm E, Lagerqvist B, et al. Mechanisms behind the prognostic value of troponin T in unstable coronary artery disease: a FRISC II substudy. J Am Coll Cardiol 2001;38:979–86.

54. Kerensky RA, Wade M, Deedwania P, et al. Revisiting the culprit lesion in non-Q-wave myocardial infarction. Results from the VANQWISH trial angiographic core laboratory. J Am Coll Cardiol 2002;39:1456–63.

55. Echols MR, Mahaffey KW, Banerjee A, et al. Racial differences among high-risk patients presenting with non-ST-segment elevation acute coronary syndromes (results from the SYNERGY trial). Am J Cardiol 2007;99:315–21.

56. Bugiardini R, Manfrini O, De Ferrari GM. Unanswered questions for management of acute coronary syndrome: risk stratification of patients with minimal disease or normal findings on coronary angiography. Arch Intern Med 2006;166:1391–5.

57. Neumann FJ, Kastrati A, Pogatsa-Murray G, et al. Evaluation of prolonged antithrombotic pretreatment ("cooling-off" strategy) before intervention in patients with unstable coronary syndromes: a randomized controlled trial. JAMA 2003;290:1593–9.

58. Fox KA, Poole-Wilson PA, Henderson RA, et al. Interventional versus conservative treatment for patients with unstable angina or non-ST-elevation myocardial infarction: the British Heart Foundation RITA 3 randomised trial. Randomized Intervention Trial of unstable Angina. Lancet 2002;360:743–51.

59. Roe MT, Harrington RA, Prosper DM, et al., for The Platelet Glycoprotein IIb/IIIa in Unstable Angina: Receptor Suppression Using Integrilin Therapy (PURSUIT) Trial Investigators. Clinical and therapeutic profile of patients presenting with acute coronary syndromes who do not have significant coronary artery disease. Circulation 2000;102:1101–6.

60. Effects of tissue plasminogen activator and a comparison of early invasive and conservative strategies in unstable angina and non-Q-wave myocardial infarction. Results of the TIMI IIIB trial. Thrombolysis in Myocardial Ischemia. Circulation 1994;89:1545–56.

61. Dey S, Flather MD, Devlin G, et al. Sex-related differences in the presentation, treatment and outcomes among patients with acute coronary syndromes: the Global Registry of Acute Coronary Events. Heart 2009;95:20–6.

62. McCullough PA, O'Neill WW, Graham M, et al. A prospective randomized trial of triage angiography in acute coronary syndromes ineligible for thrombolytic therapy. Results of the Medicine versus Angiography in Thrombolytic Exclusion (MATE) trial. J Am Coll Cardiol 1998;32:596–605.

63. Topol EJ, Yadav JS. Recognition of the importance of embolization in atherosclerotic vascular disease. Circulation 2000;101:570–80.

64. Arroyo LH, Lee RT. Mechanisms of plaque rupture: mechanical and biologic interactions. Cardiovasc Res 1999;41:369–75.

65. Kwong RY, Chan AK, Brown KA, et al. Impact of unrecognized myocardial scar detected by cardiac magnetic resonance imaging on event-free survival in patients presenting with signs or symptoms of coronary artery disease. Circulation 2006;113:2733–43.

66. Barbier CE, Bjerner T, Johansson L, et al. Myocardial scars more frequent than expected: magnetic resonance imaging detects potential risk group. J Am Coll Cardiol 2006;48:765–71.

67. Lloyd-Jones D, Adams R, Carnethon M, et al. Heart disease and stroke statistics—2009 update: a report from the American Heart Association Statistics Committee and Stroke Statistics Subcommittee. Circulation 2009;119:e21–181.

68. Camm AJ, Lüscher TF, Serruys PW, for the European Society of Cardiology. The ESC Textbook of Cardiovascular Medicine. Malden, MA/Oxford: Blackwell/European Society of Cardiology, 2006.

69. Kwong RY, Schussheim AE, Rekhraj S, et al. Detecting acute coronary syndrome in the emergency department with cardiac magnetic resonance imaging. Circulation 2003;107:531–7.

70. Cury RC, Shash K, Nagurney JT, et al. Cardiac magnetic resonance with T2-weighted imaging improves detection of patients with acute coronary syndrome in the emergency department. Circulation 2008; 118:837–44.

71. McCrohon JA, Moon JC, Prasad SK, et al. Differentiation of heart failure related to dilated cardiomyopathy and coronary artery disease using gadolinium-enhanced cardiovascular magnetic resonance. Circulation 2003;108:54–9.

72. Mahrholdt H, Wagner A, Judd RM, et al. Delayed enhancement cardiovascular magnetic resonance assessment of non-ischaemic cardiomyopathies. Eur Heart J 2005;26:1461–74.

73. Hunold P, Schlosser T, Vogt FM, et al. Myocardial late enhancement in contrast-enhanced cardiac MRI: distinction between infarction scar and non-infarction-related disease. AJR Am J Roentgenol 2005;184:1420–6.

74. Reimer KA, Jennings RB. The "wavefront phenomenon" of myocardial ischemic cell death. II. Transmural progression of necrosis within the framework of ischemic bed size (myocardium at risk) and collateral flow. Lab Invest 1979;40:633–44.

75. Senthilkumar A, Majmudar MD, Shenoy C, Kim HW, Kim RJ. Identifying the etiology: a systematic approach using delayed enhancement cardiovascular magnetic resonance. Heart Fail Clin 2009; 5:349–67.

76. Assomull RG, Lyne JC, Keenan N, et al. The role of cardiovascular magnetic resonance in patients presenting with chest pain, raised troponin, and unobstructed coronary arteries. Eur Heart J 2007;28: 1242–9.

77. Larson DM, Menssen KM, Sharkey SW, et al. "False-positive" cardiac catheterization laboratory activation among patients with suspected ST-segment elevation myocardial infarction. JAMA 2007; 298:2754–60.

78. Mahrholdt H, Wagner A, Holly TA, et al. Reproducibility of chronic infarct size measurement by contrast-enhanced magnetic resonance imaging. Circulation 2002;106:2322–7.

79. Thiele H, Kappl MJ, Conradi S, et al. Reproducibility of chronic and acute infarct size measurement by delayed enhancement-magnetic resonance imaging. J Am Coll Cardiol 2006;47:1641–5.

80. Gerber BL, Garot J, Bluemke DA, et al. Accuracy of contrast-enhanced magnetic resonance imaging in predicting improvement of regional myocardial function in patients after acute myocardial infarction. Circulation 2002;106:1083–9.

81. Kim RJ, Wu E, Rafael A, et al. The use of contrast-enhanced magnetic resonance imaging to identify reversible myocardial dysfunction. N Engl J Med 2000;343:1445–53.

82. Kuhl HP, Lipke CS, Krombach GA, et al. Assessment of reversible myocardial dysfunction in chronic ischaemic heart disease: comparison of contrast-enhanced cardiovascular magnetic resonance and a combined positron emission tomography-single photon emission computed tomography imaging protocol. Eur Heart J 2006;27:846–53.

83. Bello D, Shah DJ, Farah GM, et al. Gadolinium cardiovascular magnetic resonance predicts reversible myocardial dysfunction and remodeling in patients with heart failure undergoing beta-blocker therapy. Circulation 2003;108:1945–53.

84. Ito H, Maruyama A, Iwakura K, et al. Clinical implications of the 'no reflow' phenomenon. A predictor of complications and left ventricular remodeling in reperfused anterior wall myocardial infarction. Circulation 1996;93:223–8.

85. Morishima I, Sone T, Okumura K, et al. Angiographic no-reflow phenomenon as a predictor of adverse long-term outcome in patients treated with percutaneous transluminal coronary angioplasty for first acute myocardial infarction. J Am Coll Cardiol 2000;36:1202–9.

86. Wu KC, Zerhouni EA, Judd RM, et al. Prognostic significance of microvascular obstruction by magnetic resonance imaging in patients with acute myocardial infarction. Circulation 1998;97:765–72.

87. Hombach V, Grebe O, Merkle N, et al. Sequelae of acute myocardial infarction regarding cardiac structure and function and their prognostic significance as assessed by magnetic resonance imaging. Eur Heart J 2005;26:549–57.

88. Kumar A, Abdel-Aty H, Kriedemann I, et al. Contrast-enhanced cardiovascular magnetic resonance imaging of right ventricular infarction. J Am Coll Cardiol 2006;48:1969–76.

89. Taylor AM, Dymarkowski S, Verbeken EK, et al. Detection of pericardial inflammation with late-enhancement cardiac magnetic resonance imaging: initial results. Eur Radiol 2006;16:569–74.

90. Mollet NR, Dymarkowski S, Volders W, et al. Visualization of ventricular thrombi with contrast-enhanced magnetic resonance imaging in patients with ischemic heart disease. Circulation 2002;106: 2873–6.

91. Srichai MB, Junor C, Rodriguez LL, et al. Clinical, imaging, and pathological characteristics of left ventricular thrombus: a comparison of contrast-enhanced magnetic resonance imaging, transthoracic echocardiography, and transesophageal echocardiography with surgical or pathological validation. Am Heart J 2006;152:75–84.

92. Weinsaft JW, Kim HW, Shah DJ, et al. Detection of left ventricular thrombus by delayed-enhancement cardiovascular magnetic resonance prevalence and markers in patients with systolic dysfunction. J Am Coll Cardiol 2008;52:148–57.

93. Gibbons RJ, Miller TD, Christian TF. Infarct size measured by single photon emission computed tomographic imaging with (99m)Tc-sestamibi: a measure of the efficacy of therapy in acute myocardial infarction. Circulation 2000;101:101–8.

94. Risk stratification and survival after myocardial infarction. N Engl J Med 1983;309:331–6.

95. Burns RJ, Gibbons RJ, Yi Q, et al. The relationships of left ventricular ejection fraction, end-systolic volume index and infarct size to six-month mortality after hospital discharge following myocardial infarction treated by thrombolysis. J Am Coll Cardiol 2002; 39:30–6.

96. Roes SD, Kelle S, Kaandorp TA, et al. Comparison of myocardial infarct size assessed with contrast-enhanced magnetic resonance imaging and left ventricular function and volumes to predict mortality in patients with healed myocardial infarction. Am J Cardiol 2007; 100:930–6.

97. Wu E, Ortiz JT, Tejedor P, et al. Infarct size by contrast enhanced cardiac magnetic resonance is a stronger predictor of outcomes than left ventricular ejection fraction or end-systolic volume index: prospective cohort study. Heart 2008;94:730–6.

98. Kwon DH, Halley CM, Carrigan TP, et al. Extent of left ventricular scar predicts outcomes in ischemic cardiomyopathy patients with significantly reduced systolic function: a delayed hyperenhancement cardiac magnetic resonance study. J Am Coll Cardiol Img 2009;2: 34–44.

99. Fieno DS, Hillenbrand HB, Rehwald WG, et al. Infarct resorption, compensatory hypertrophy, and differing patterns of ventricular remodeling following myocardial infarctions of varying size. J Am Coll Cardiol 2004;43:2124–31.

100. Rochitte CE, Lima JA, Bluemke DA, et al. Magnitude and time course of microvascular obstruction and tissue injury after acute myocardial infarction. Circulation 1998;98:1006–14.

101. Bondarenko O, Beek AM, Hofman MB, et al. Standardizing the definition of hyperenhancement in the quantitative assessment of

infarct size and myocardial viability using delayed contrast-enhanced CMR. J Cardiovasc Magn Reson 2005;7:481–5.

102. Heiberg E, Ugander M, Engblom H, et al. Automated quantification of myocardial infarction from MR images by accounting for partial volume effects: animal, phantom, and human study. Radiology 2008;246:581–8.

103. Hsu LY, Ingkanisorn WP, Kellman P, et al. Quantitative myocardial infarction on delayed enhancement MRI. Part II: clinical application of an automated feature analysis and combined thresholding infarct sizing algorithm. J Magn Reson Imaging 2006;23:309–14.

104. Hsu LY, Natanzon A, Kellman P, et al. Quantitative myocardial infarction on delayed enhancement MRI. Part I: animal validation of an automated feature analysis and combined thresholding infarct sizing algorithm. J Magn Reson Imaging 2006;23:298–308.

105. Kellman P, Chung YC, Simonetti OP, et al. Multi-contrast delayed enhancement provides improved contrast between myocardial infarction and blood pool. J Magn Reson Imaging 2005;22:605–13.

106. Bulow H, Klein C, Kuehn I, et al. Cardiac magnetic resonance imaging: long term reproducibility of the late enhancement signal in patients with chronic coronary artery disease. Heart 2005;91:1158–63.

107. Fleiss JL. The Design and Analysis of Clinical Experiments. New York, NY: Wiley, 1986.

108. Ibrahim T, Nekolla SG, Hornke M, et al. Quantitative measurement of infarct size by contrast-enhanced magnetic resonance imaging early after acute myocardial infarction: comparison with single-photon emission tomography using Tc99m-sestamibi. J Am Coll Cardiol 2005;45:544–52.

109. Lunde K, Solheim S, Aakhus S, et al. Intracoronary injection of mononuclear bone marrow cells in acute myocardial infarction. N Engl J Med 2006;355:1199–209.

110. ClinicalTrials.gov List Results. Available at: http://clinicaltrials.gov/ct2/results?term=infarct+size&pg=1. Accessed March 3, 2009.

111. Piot C, Croisille P, Staat P, et al. Effect of cyclosporine on reperfusion injury in acute myocardial infarction. N Engl J Med 2008;359:473–81.

112. Thiele H, Schindler K, Friedenberger J, et al. Intracoronary compared with intravenous bolus abciximab application in patients with ST-elevation myocardial infarction undergoing primary percutaneous coronary intervention: the randomized Leipzig immediate percutaneous coronary intervention abciximab IV versus IC in ST-elevation myocardial infarction trial. Circulation 2008;118:49–57.

113. Sardella G, Mancone M, Bucciarelli-Ducci C, et al. Thrombus aspiration during primary percutaneous coronary intervention improves myocardial reperfusion and reduces infarct size: the EXPIRA (thrombectomy with export catheter in infarct-related artery during primary percutaneous coronary intervention) prospective, randomized trial. J Am Coll Cardiol 2009;53:309–15.

114. Atar D, Petzelbauer P, Schwitter J, et al. Effect of intravenous FX06 as an adjunct to primary percutaneous coronary intervention for acute ST-segment elevation myocardial infarction. J Am Coll Cardiol 2009;53:720–9.

▶ **APPENDIX**

For Online Figure 1, please see the online version of this article.